

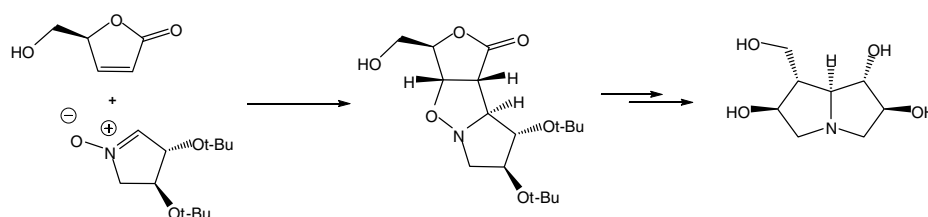
Contents

FULL PAPERS

Synthesis of pyrrolizidine alkaloids via 1,3-dipolar cycloaddition involving cyclic nitrones and unsaturated lactones

pp 2215–2220

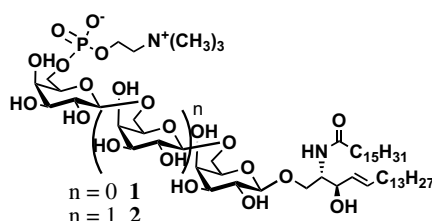
Sebastian Stecko, Margarita Jurczak, Zofia Urbańczyk-Lipkowska, Jolanta Solecka and Marek Chmielewski*



Synthetic studies on glycosphingolipids from Protostomia phyla: syntheses and biological activities of amphoteric glycolipids containing a phosphocholine residue from the earthworm *Pheretima hilgendorfi*

pp 2221–2228

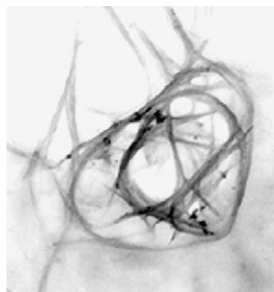
Noriyasu Hada,* Yukihiro Shida, Hiroshi Shimamura, Yoshiko Sonoda, Tadashi Kasahara, Mutsumi Sugita and Tadahiro Takeda*



Detergency effects of nanofibrillar amyloid formation on glycation of human serum albumin

pp 2229–2234

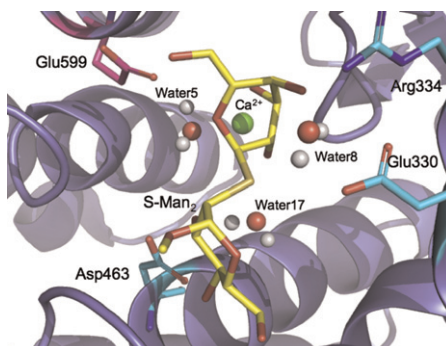
Naghmeh Sattarahmady, Ali A. Moosavi-Movahedi,* Mehran Habibi-Rezaei, Shahin Ahmadian, Ali A. Saboury, Hossein Heli and Nader Sheibani



Nanofibrillar amyloid of glycated HSA

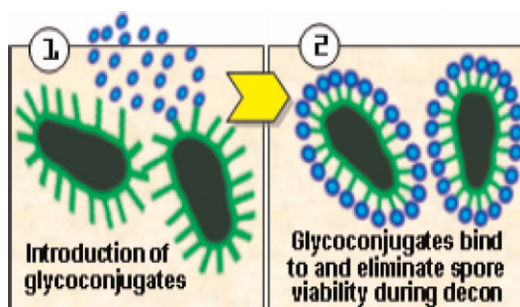
Theory and computation show that Asp463 is the catalytic proton donor in human endoplasmic reticulum α -(1 \rightarrow 2)-mannosidase I pp 2235–2242

David Cantú, Wim Nerinckx and Peter J. Reilly*



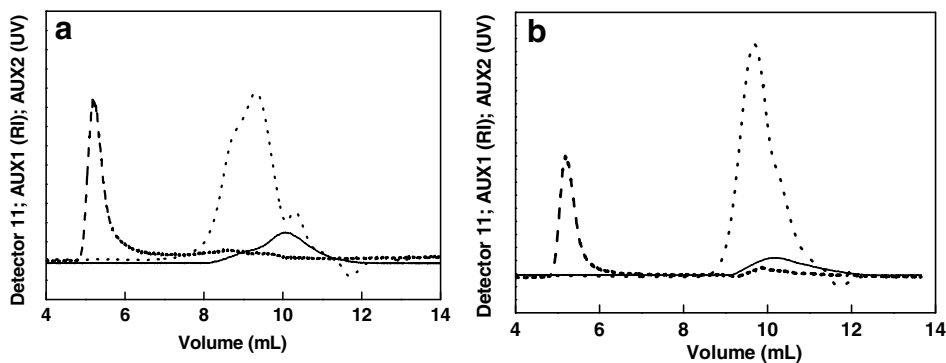
Defensive and simultaneous actions of glycoconjugates during spore decontamination pp 2243–2250

Olga Tarasenko,* Samea Lone and Pierre Alusta



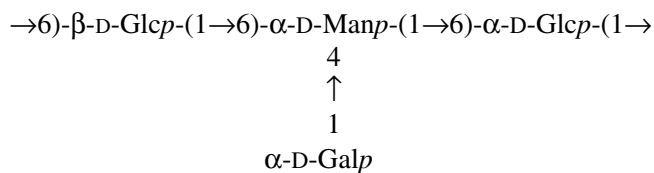
Characterization of polysaccharide–protein complexes by size-exclusion chromatography combined with three detectors pp 2251–2257

Yongzhen Tao and Lina Zhang*



NMR and MALDI-TOFMS analysis of a heteroglycan isolated from hot water extract of edible mushroom, *Volvariella bombycina* pp 2258–2265

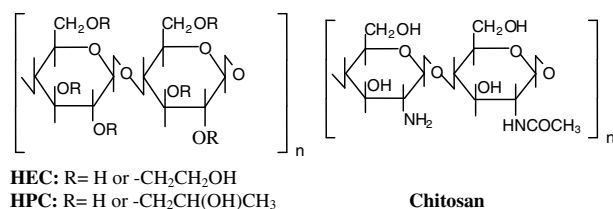
Debsankar Das, Debabrata Maiti, Krishnendu Chandra, Subhas Mondal, Arnab K. Ojha, Sadhan K. Roy, Kaushik Ghosh and Syed S. Islam*



Calculation of viscometric constants, hydrodynamic volume, polymer–solvent interaction parameter, and expansion factor for three polysaccharides with different chain conformations

pp 2266–2277

Mohammad R. Kasaai

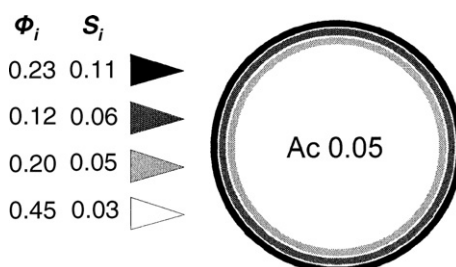


Calculation of several parameters (K ; a ; K_θ ; α ; B ; and $[\eta]M_v$) for three polysaccharides using: (1) $[\eta] = K \cdot M_v^a$; (2) $[\eta] = K_\theta \cdot M^{1/2}\alpha^3$; (3) $[\eta] = K_\theta \cdot M_v^{0.5} + 0.51 \cdot B \cdot M_v$.

Surface effects in the acetylation of granular potato starch

pp 2278–2284

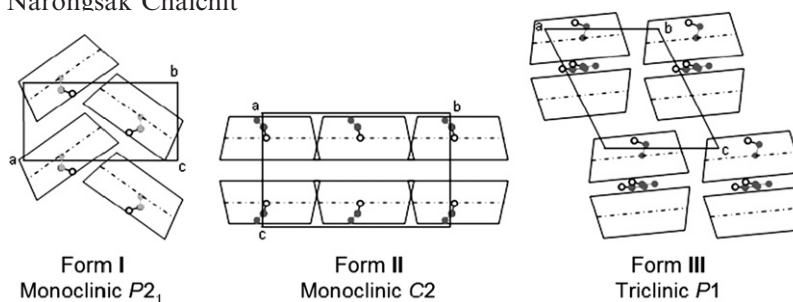
Peter A. M. Steeneken* and Albert J. J. Woortman



Crystal form III of β -cyclodextrin–ethanol inclusion complex: layer-type structure with dimeric motif

pp 2285–2291

Thammarat Aree* and Narongsak Chaichit

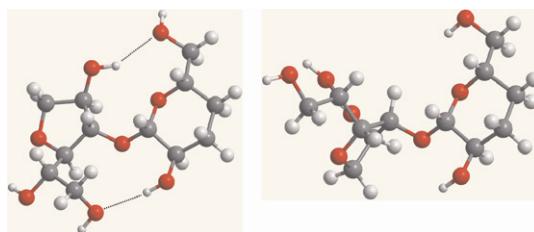


Pseudopolymorphism in the β -CD–EtOH inclusion complex is depicted as a distinction in crystal packing modes.

DFT/MM modeling of the five-membered ring in 3,6-anhydrogalactose derivatives and its influence on disaccharide adiabatic maps

pp 2292–2298

Diego A. Navarro and Carlos A. Stortz*



^{13}C CP MAS NMR and crystal structure of methyl glycopyranosides

pp 2299–2307

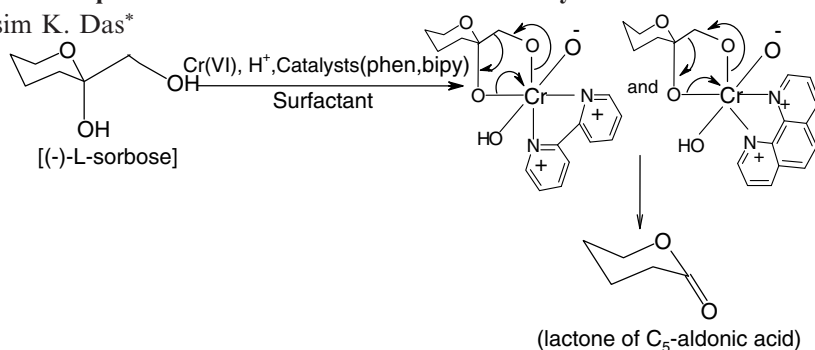
Katarzyna Paradowska, Tomasz Gubica, Andrzej Temeriusz,* Michał K. Cyrański and Iwona Wawer

The X-ray diffraction analysis, ^{13}C CP MAS NMR spectra and powder X-ray diffraction patterns were obtained for selected methyl glycosides: α - and β -D-lyxopyranosides (**1**, **2**), α - and β -L-arabinopyranosides (**3**, **4**), α - and β -D-xylopyranosides (**5**, **6**) and β -D-ribose (**7**), and the results were confirmed by GIAO DFT calculations of shielding constants. The powder X-ray diffraction (PXRD) performed for **4**, **5** and **7** revealed that the sample of **7** existed as a mixture of two polymorphs, and one of them probably consisted of two non-equivalent molecules.

Heteroaromatic N-base ligands in 1,10-phenanthroline- and 2,2'-bipyridyl-assisted chromic acid oxidation of (–)-L-sorbose in aqueous micellar acid media: a kinetic study

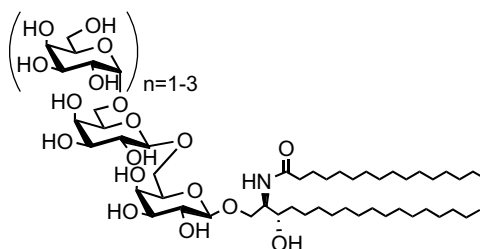
pp 2308–2314

Monirul Islam and Asim K. Das*

**NOTES****Synthesis of neutral glycosphingolipids from *Zygomycetes***

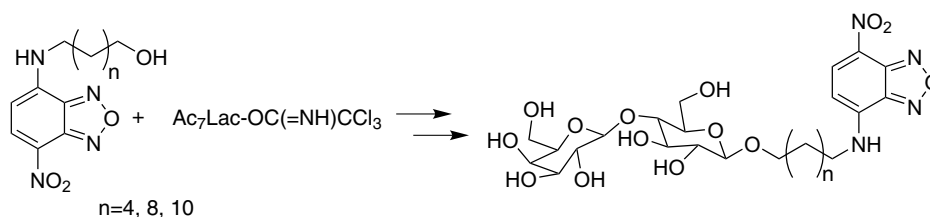
pp 2315–2324

Noriyasu Hada, Junko Oka, Kyoko Hakamata, Kenji Yamamoto and Tadahiro Takeda*

**Synthesis of fluorescent alkyl lactoside derivatives**

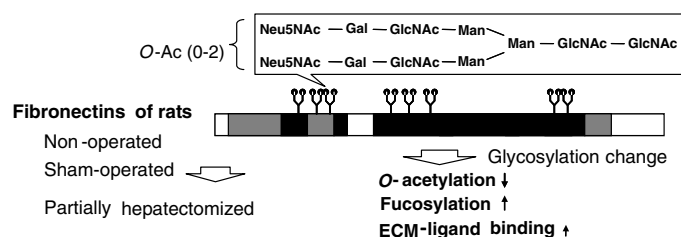
pp 2325–2328

Soichiro Watanabe



Glycosylation and ligand-binding activities of rat plasma fibronectin during liver regeneration after partial hepatectomy pp 2329–2335

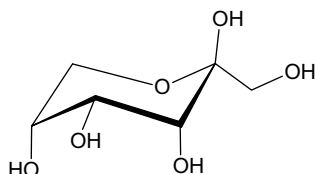
Kotone Sano, Miho Asahi, Maiko Yanagibashi, Noritaka Hashii, Satsuki Itoh, Nana Kawasaki and Haruko Ogawa*



Crystal structure of β -D-psicopyranose

Anna Kwiecień,* Katarzyna Ślepokura and Tadeusz Lis

pp 2336–2339



*Corresponding author

i+ Supplementary data available via ScienceDirect

COVER

The graphic represents a molecular dynamics simulation of water density around the disaccharide α -D-Araf-(1 \rightarrow 5)- α -D-Araf-OCH₃, highlighting the interglycosidic linkage. The red clouds represent regions where the probability of finding an oxygen atom is high while the gray clouds are for hydrogen atoms. This work is the result of a collaboration in the Alberta Ingenuity Centre for Carbohydrate Science and Department of Chemistry at the University of Alberta between the groups of Pierre-Nicolas Roy and Todd L. Lowary (Castillo, N.; Roy, P. N.; Lowary, T. L. Manuscript in Preparation).
© 2008 T. L. Lowary. Published by Elsevier Ltd.

Available online at www.sciencedirect.com



Abstracted/Indexed in: Chem. Abstr.: Curr. Contents: Phys., Chem. & Earth Sci. Life Sci. Current Awareness in Bio. Sci. (CABS). Science Citation Index. Full texts are incorporated in CJELSEVIER, a file in the Chemical Journals Online database which is available on STN® International. Also covered in the abstract and citation database SCOPUS®. Full text available on ScienceDirect®



ELSEVIER

ISSN 0008-6215